Transport and Communications Science Journal

SEISMIC ANALYSIS OF A SOIL-LIQUID TANK SYSTEM USING THE TWO-STEP METHOD

Huynh Van Quan

Campus in Ho Chi Minh City, University of Transport and Communications, No. 450-451 Le Van Viet Street, Tang Nhon Phu A Ward, Thu Duc, Ho Chi Minh City, Vietnam

ARTICLE INFO

TYPE: Research Article
Received: 14/05/2023
Revised: 16/12/2023
Accepted: 26/01/2024
Published online: 15/05/2024
https://doi.org/10.47869/tcsj.75.4.2

Corresponding author
Email: quanhv_ph@utc.edu.vn; Tel: +84986503205

Abstract. Seismic analysis of soil-structure interaction (SSI) is a challenge due to the non-linearities of soil-foundation interaction (SFI). The reliability of the design and the analysis results will suffer if SSI is ignored. In this paper, a two-step method based on the superposition theorem is used to perform a seismic analysis of a soil-foundation-tank-liquid system (soil-liquid tank system). The SFI analysis was conducted in the first step using the CyclicTP program's finite-element method. Meanwhile, the liquid tank system was analyzed in the second step using the lumped-parameter method. Numerical simulations conducted in homogeneous strata of sand soil demonstrated that the responses of the liquid tank were 24–70% higher than the results of the fixed-base model. Compared to the sway-rocking model, these responses did not differ by 20%. This study also investigated cohesive soils of homogeneous clays and multiple strata. The paper recommends that future research investigate the experimentation, the geometric nonlinearity of the soil-foundation system, and the stress-strain analysis of the tank wall.

Keywords: liquid tank system, soil-foundation interaction, soil-structure interaction, seismic analysis, superposition theorem.

1. INTRODUCTION

Most seismic analyses for structural design are carried out with the assumption that the structures are fixed at the foundation level, as illustrated by Fig. 1(a), the fixed-base model [1]. Inertial forces produced by an earthquake's loading cause base shears and bending moments at the structure's base. The base of the structure can rotate and translate at the structural base, as shown in Fig. 1(b), the sway-rocking model [2]. In this model, the structure is connected at the base by rotational and horizontal springs. In highly flexible structural systems, foundation motions may be neglected due to their small value in relation to the structure. However, for stiff structures, the overall flexibility of the system may be greatly increased by foundation motions. Therefore, ignoring these effects could make seismic response estimations unreliable [3].

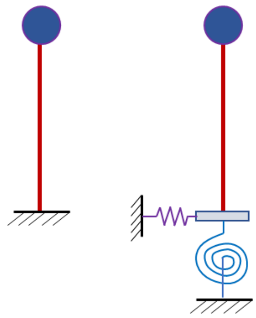

Figure 1. Two available simplified models: (a) fixed-base model [1], (b) sway-rocking model [2].

Seismic waves from an earthquake are transmitted from the ground through a structure's foundations. The structure is excited when seismic waves hit the foundations. The motion of the structure simultaneously changes the movement of the foundation and ground. The term "soil-structure interaction" refers to this phenomenon. The dynamically excited structure at a soil site causes two phenomena: kinematic and inertial interactions. Seismic analysis in the absence of a structure is referred to as kinematic interaction. Incoming seismic waves are reflected and refracted as they approach the soil-foundation interface because the foundation's stiffness is different from that of the nearby soil. The second phenomenon, inertial interaction, takes place when a structure is dynamically excited by a kinematic interaction [2,4].

The seismic interaction of soil-foundation systems was simply modeled using commercial software in the case of liquid tanks analyzed using the finite element method (FEM). Using the SAP2000 and 3DBASIS-ME programs, Seleemah [5,6] examined the seismic response of liquid tanks isolated by elastomeric or sliding bearings. Livaoglu [7] studied the effects of foundation placement on liquid tank responses, with a focus on soft soils and tank roofs. The ANSYS program was used to perform the dynamic analysis of the interaction between soil, foundation, tank, and liquid (SFTL). In Zhang's research [8], the SFTL system was also numerically simulated using the ANSYS program.

Many studies (e.g., Quan [9], Saha [10], Miguel [11], Kim [12], and Malhotra [13]) have investigated the seismic response of liquid tanks under the assumption that the foundations are fixed to the ground. As seen in Fig. 2(a), the tanks in other investigations were isolated from the foundation. For instance, Shrimali [14-16] created a series of papers using modal analysis, various tank aspect ratios, and bearing properties to determine the response of base-isolated liquid tanks.

A substructure method and a hybrid method for SFI have been typically combined with the most popular lumped-parameter model (LPM) for liquid tanks, which have been described in several design standards (e.g., API 650 [17], NZSEE [18]). The time-history responses of SFTL systems were obtained by Farajian [19]. As shown in Fig. 2(b), the study used the coupled spring-damper model of SFI and the simplified mass-spring model of the liquid tank. The motion equations were simulated using a MATLAB program. Larkin [20,21] obtained the responses of liquid tanks by simulating the SFI using a sway-rocking model, see Fig. 2(c). According to Larkin's results, shear forces and overturning moments in soft soils are especially impacted by SSI. For the seismic analysis of horizontal tanks, Lyu [22] used a simplified mechanical SFI model with three degrees of freedom, see Fig. 2(d). According to the study, horizontal tank responses to seismic loadings and the effects of soft and medium soils increased by 25–58%.

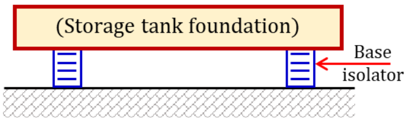

(a) Base-isolated tank model [10-12]

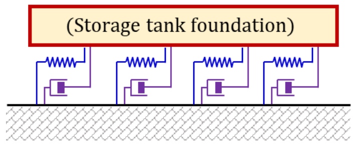

(b) Coupled spring-damper model [19]

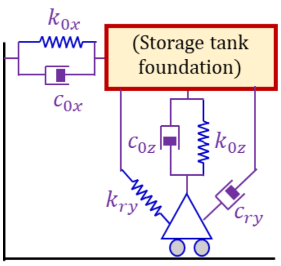

(c) Sway-rocking model [20,21]

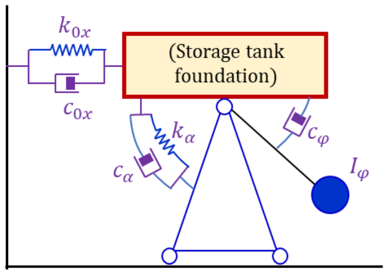

(d) Sway-rocking model [22]

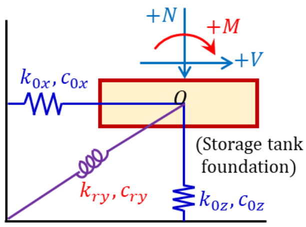

(e) Macro-element model [23,24]

Figure 2. The models of soil-foundation interaction.

In Vietnam, Quan [23,24] combined the simple LPM of a liquid tank with the macro-element model of a hybrid method to simulate SFI; see Fig. 2(e). Quan [25], see Fig. 3, used the sway-rocking model in Fig. 2(d) to analyze a vertical cylindrical liquid storage tank subjected to seismic loads.

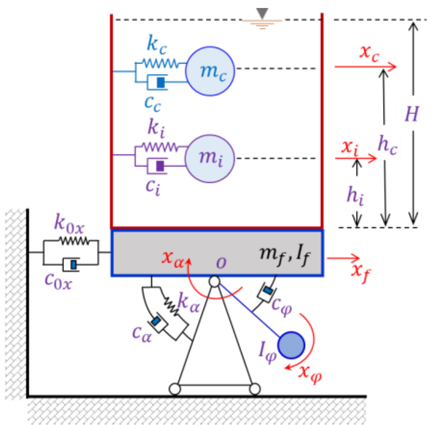

Figure 3. A simulation of SFTL with sway-rocking model [25].

As was previously mentioned, the FEM and LPM can be used to simulate SFI. Simulating SFI non-linearities with FEM software such as ANSYS, SAP2000, 3DBASIS-ME, etc., requires a significant amount of computation. Nowadays, specialized software (like CyclicTP and OpenSeesPL [26]) can be used to complete this challenging and complex task. Separate analyses of the structure and soil-foundation system are necessary to apply the superposition theorem [27]. So, this paper proposes that the dynamic analysis of SFTL systems be solved using a combination of FEM and LPM.

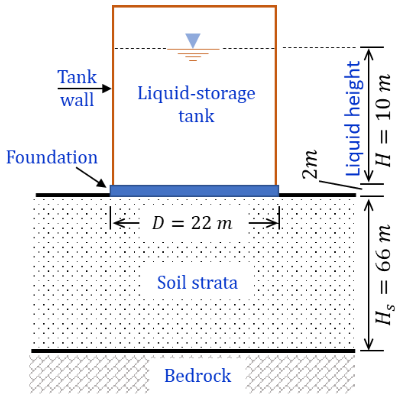

Figure 4. An illustration of soil, foundation, and liquid tank system.

In view of the above, this paper proposes a simple approach for seismic analysis of an SFTL. CyclicTP is used to identify the kinematic interactions of SFI. The analysis of LTI, which determines the inertial interaction, uses the first step's results as input. The main focus of this paper is to investigate how SSI affects the seismic response of the SFTL system depicted in Fig. 4. The analysis results of the proposed method are compared to sway-rocking (shown in Fig. 3) and fixed-base models. The paper also investigates the different types of homogeneous ground (sand and clay) and multiple strata.

2. TWO-STEP METHOD FOR SEISMIC ANALYSIS OF LIQUID TANK SYSTEMS

According to Kausel's superposition theorem [4], the SSI analysis was carried out in two steps, as shown in Fig. 5. The matrix Eq. (1) contains the general equations of motion for the analyzed system. Where $\boldsymbol{u}$ and $\boldsymbol{y}$ are the absolute and relative displacements; $\boldsymbol{M}$, $\boldsymbol{C}$ and $\boldsymbol{K}$ are the system mass, damping and stiffness matrices, respectively.

$$\boldsymbol{M}\ddot{\boldsymbol{u}} + \boldsymbol{C}\dot{\boldsymbol{y}} + \boldsymbol{K}\boldsymbol{y} = 0 \tag{1}$$

The solution of Eq. (1) is equivalent to the resolution of two matrices:

$$\boldsymbol{M_1}\ddot{\boldsymbol{u}}_1 + \boldsymbol{C}\dot{\boldsymbol{y}}_1 + \boldsymbol{K}\boldsymbol{y}_1 = 0 \tag{2}$$

and

$$\boldsymbol{M}\ddot{\boldsymbol{u}}_2 + \boldsymbol{C}\dot{\boldsymbol{y}}_2 + \boldsymbol{K}\boldsymbol{y}_2 = -\boldsymbol{M}_2\ddot{\boldsymbol{u}}_1 \tag{3}$$

where $(\boldsymbol{y}_1, \ \boldsymbol{u}_1)$ and $(\boldsymbol{y}_2, \ \boldsymbol{u}_2)$ are the relative and absolute displacements of the foundation and structure, respectively; $\boldsymbol{u}_g$ is the ground motion vector; $\boldsymbol{M}_1$ excludes the mass of the structure, while $\boldsymbol{M}_2$ excludes the mass of the soil. $\boldsymbol{u}_1 = \boldsymbol{y}_1 + \boldsymbol{u}_g$, $\boldsymbol{u} = \boldsymbol{u}_1 + \boldsymbol{y}_2$, $\boldsymbol{y} = \boldsymbol{y}_1 + \boldsymbol{y}_2$ and $\boldsymbol{M} = \boldsymbol{M}_1 + \boldsymbol{M}_2$.

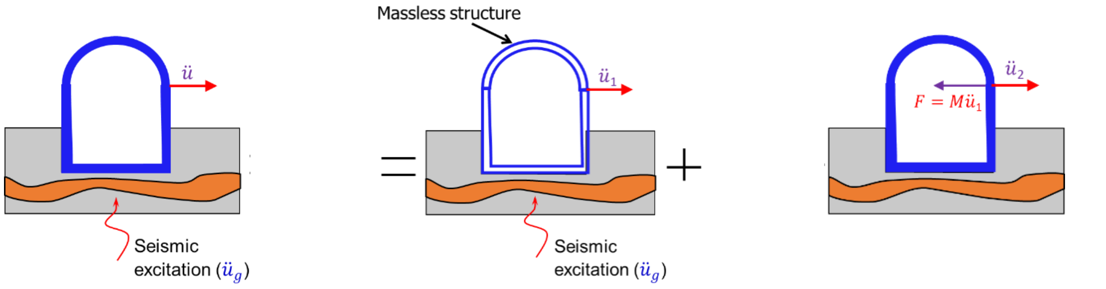

(a) The complete solution

(b) The first step-kinematic interaction

(c) The second step-inertial interaction

Figure 5. Two steps of the SSI problem using superposition theorem [4].

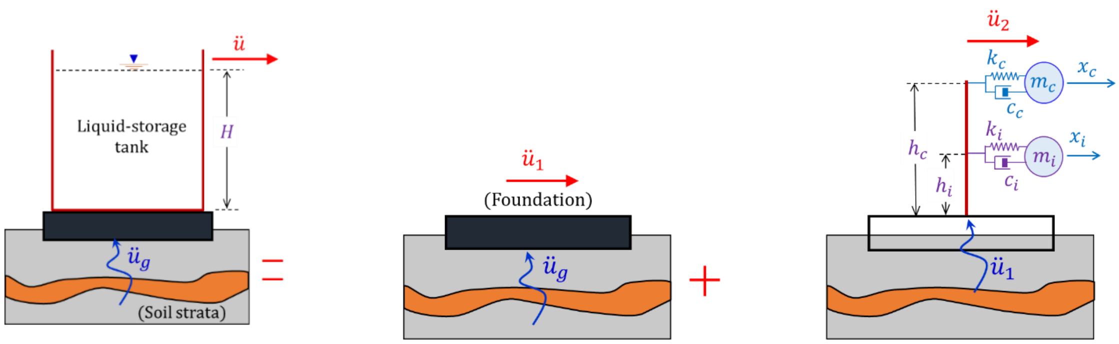

(a) Analytical results $\ddot{\boldsymbol{u}}$

(b) The first step result ($\ddot{\boldsymbol{u}}_1$)-kinematic interaction

(c) The second step result ($\ddot{\boldsymbol{u}}_2$)-inertial interaction

Figure 6. Seismic analysis of a liquid tank system using two-step method.

The response of the massless structure is obtained in the first step by resolving Eq. (2). Next, Eq. (3) of the second step is solved by applying inertia forces to the structure using the results of the first step as the input parameters. Kinematic and inertial interactions, respectively, are terms used to describe the analytical results of the first and second steps. In this paper, the analytical solution using Kausel's proposal is called a two-step method from now on.

The proposed analysis procedure is shown in Figs. 6(b-c) when a liquid tank located on a soil stratum is subjected to seismic loading following the two-step method. The system of soil and tank foundation under seismic loading ($\ddot{\boldsymbol{u}}_g$) are analyzed in the first step, Fig. 6(b), to determine the acceleration of the foundation ($\ddot{\boldsymbol{u}}_1$). The model of the liquid tank under excitation $\ddot{\boldsymbol{u}}_1$ is examined in the second step, Fig. 6(c), to determine the liquid tank responses ($\ddot{\boldsymbol{u}}_2$).

The kinematic interaction ($\ddot{\boldsymbol{u}}_1$) can now be performed by available software or by a script written in a programming language, such as MATLAB. SFI's non-linearities are challenging for researchers who aren't skilled programmers. However, these tasks are resolved by the free software CyclicTP for shallow foundations, which has been used in many studies [28–31]. The first step in this study is simulated by CyclicTP (version Beta 0.3.0, updated October 23, 2015) [26], while the second step is simulated by LPM, which is based on the API 650 model [17].

The entire liquid mass (m) of the tank vibrates in two different ways [17]: convective and impulsive masses. The convective mass (m_c), the top liquid mass, alters the free liquid surface.

The impulsive mass (m_i), the intermediate liquid mass, vibrates simultaneously with the tank wall [9]. Eqs. (4)-(8) are used to express the different masses, centroid heights of masses, and associated vibration periods of the liquid-tank system [7].

$$\begin{cases} m_c = 0.230\frac{D}{H}m\tanh\left(\frac{3.67H}{D}\right) \\ h_c = \left(1 - \frac{\cosh\left(\frac{3.67H}{D}\right)-1}{\frac{3.67H}{D}\sinh\left(\frac{3.67H}{D}\right)}\right)H \end{cases} \tag{4}$$

For $D/H \geq 1.333$ (broad tanks):

$$\begin{cases} m_i = \frac{\tanh\left(0.866\frac{D}{H}\right)}{0.866\frac{D}{H}}m \\ h_i = 0.375H \end{cases} \tag{5}$$

For $D/H < 1.333$ (slender tanks):

$$\begin{cases} m_i = \left(1 - 0.218\frac{D}{H}\right)m \\ h_i = \left(0.5 - 0.094\frac{D}{H}\right)H \end{cases} \tag{6}$$

$$T_i = \frac{2\pi}{\omega_i} = C_i\frac{H\sqrt{\rho}}{\sqrt{\frac{2t}{D}}\times\sqrt{E}} \tag{7}$$

$$T_c = \frac{2\pi}{\omega_c} = C_c\sqrt{D} \tag{8}$$

where H is the liquid height, R and D are the radius and diameter of the liquid tank, ρ is the liquid density, E is the Young's modulus for tank material, t is the equivalent uniform thickness of the tank wall, and T_i and T_c are the natural periods of the impulsive and convective responses, respectively. The impulsive and convective coefficients, C_i and C_c, can be looked up on a data table or diagram that is readily available [5]. The coefficient C_i is dimensionless, while C_c is expressed in $s/\sqrt{m}$. The sloshing and impulsive masses are connected to the tank wall by corresponding equivalent springs and dampers; having stiffness and viscous damping $k_c = m_c\omega_c^2$, $c_c = 2\xi_c m_c\omega_c$ and $k_i = m_i\omega_i^2$, $c_i = 2\xi_i m_i\omega_i$ respectively.

The liquid tank, as shown in Fig. 5(c), has two degrees of freedom (DOF). Under foundation excitation ($\ddot{u}_1$), Eqs. (9) and (10) are the basic equations of motion and are expressed in matrix form as Eq. (11). Only horizontal responses are studied in this paper (x_c, x_i). A MATLAB-Simulink tool diagram is used to resolve Eq. (11) as shown in Fig. 7. In the following sections, the numerical calculations from the proposal are compared with the fixed-base and sway-rocking models.

$$m_c\ddot{x}_c + c_c\dot{x}_c + k_c x_c = m_c\ddot{u}_1 \tag{9}$$

$$m_i\ddot{x}_i + c_i\dot{x}_i + k_i x_i = m_i\ddot{u}_1 \tag{10}$$

$$\begin{bmatrix} m_c & 0 \\ 0 & m_i \end{bmatrix}\begin{Bmatrix} \ddot{x}_c \\ \ddot{x}_i \end{Bmatrix} + \begin{bmatrix} c_c & 0 \\ 0 & c_i \end{bmatrix}\begin{Bmatrix} \dot{x}_c \\ \dot{x}_i \end{Bmatrix} + \begin{bmatrix} k_c & 0 \\ 0 & k_i \end{bmatrix}\begin{Bmatrix} x_c \\ x_i \end{Bmatrix} = \begin{bmatrix} m_c & 0 \\ 0 & m_i \end{bmatrix}\ddot{u}_1 \tag{11}$$

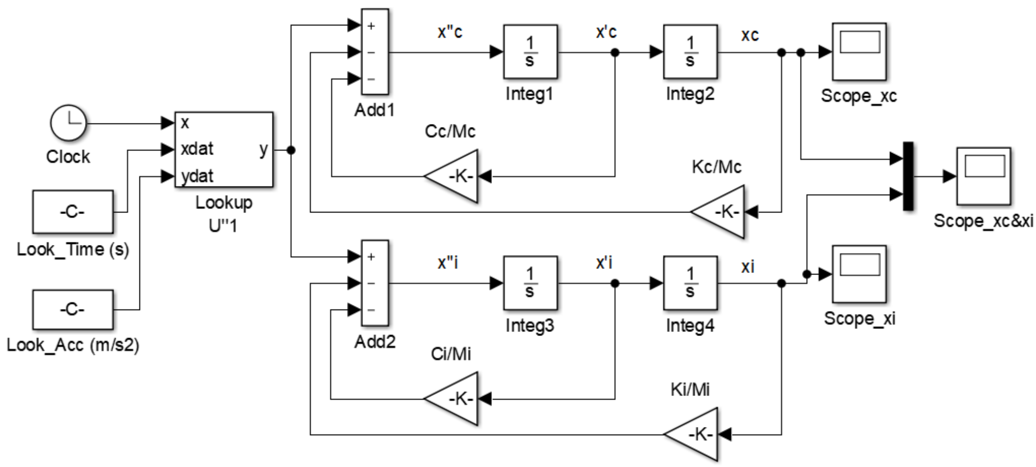

Figure 7. Diagram using MATLAB-Simulink to solve Eq. (11).

3. NUMERICAL ANALYSIS AND RESULTS

3.1. Description of storage tank system and ground motion

The geometric characteristics of a cylindrical tank model are as follows: tank radius $R = D/2 = 10$ m, liquid height $H = 10$ m, $D/H = 2.0$, equivalent uniform thickness of the tank wall $t = 15$ mm, and Young's modulus of steel $E = 200$ GPa. The reinforced concrete shallow circular foundation has a 2 m depth above the surface, a radius of $R_b = R + 1 = 11$ m [16], and a density of $\rho_c = 2.1\times10^3$ kg/m^3. Water is added to the tank at a density of $\rho = 1.0\times10^3$ kg/m^3. Table 1 lists the parameters for the liquid tank model's impulsive and convective vibration modes.

Table 1. The resultant parameters of the equivalent mechanical model of liquid tank [23].

m_c (kg)	m_i (kg)	C_c $\left(s/\sqrt{m}\right)$	C_i	T_c (s)	T_i (s)
14.19×10^5	17.21×10^5	1.52	6.36	6.80	0.12
h_c (m)	h_i (m)	k_c (N/m)	k_i (N/m)	c_c (Ns/m)	c_i (Ns/m)
6.16	4.19	12.11×10^5	4.71×10^9	13.11×10^5	3.60×10^8

Table 2. Basic model parameter values of soils [32,33].

Soil type	Shear wave velocity (m/s)	Friction angle/ Undrained shear strength (kPa)	Possion's ratio	Mass density (kg/m^3)	Permeability coeff. (m/s)
Dense sand	255	40^o	0.4	2.1×10^3	6.6×10^{-5}
Medium clay	200	37.0	0.4	1.5×10^3	1.0×10^{-9}
Stiff clay	300	75.0	0.4	1.8×10^3	1.0×10^{-9}

This study examines the heavy soil types that are suitable for shallow foundations and are similar to the fixed-base model. Table 2 is a list of the predefined parameters of the soils, these are the CyclicTP defaults. The soil profile is a homogeneous stratum, see Fig. 4. The soil depth $H_s = 66$ m is meshed into a stratum with 66 layers from the top to the bottom. With the non-linear analysis option, CyclicTP creates a mesh with 4402 nodes and 1056 elements. The equivalent parameters of the soil-foundation system in the sway-rocking model are listed in Table 3.

Table 3. Equivalent soil-foundation system parameters for the sway-rocking model [25].

m_f (kg)	I_f (kgm^2)	k_H (N/m)	c_H (Ns/m)
1.4×10^6	43.37×10^6	8.53×10^9	3.28×10^8
k_α (Nm/rad)	c_α (Nms/rad)	c_φ (Nms/rad)	I_φ (kgm^2)
1.06×10^{12}	7.23×10^6	18.36×10^9	6.56×10^8

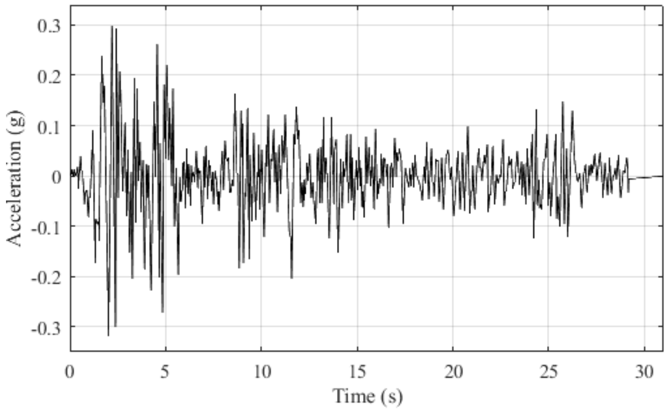

Figure 8. The acceleration time history of the earthquake of El Centro (1940) [34].

Fig. 8 depicts the time history of ground accelerations during the El Centro (1940) earthquake, with $PGA = 0.319g$ and gravity acceleration $g = 9.81$ m/s^2 [34]. Due to the complete collection of input motion data, this famous earthquake has been included in popular textbooks such as [35]. As seen in Fig. 9(a), the ground motion of this earthquake ($\ddot{\boldsymbol{u}}_g$) is applied longitudinally to the structure in the Input Motion section of CyclicTP's main window.

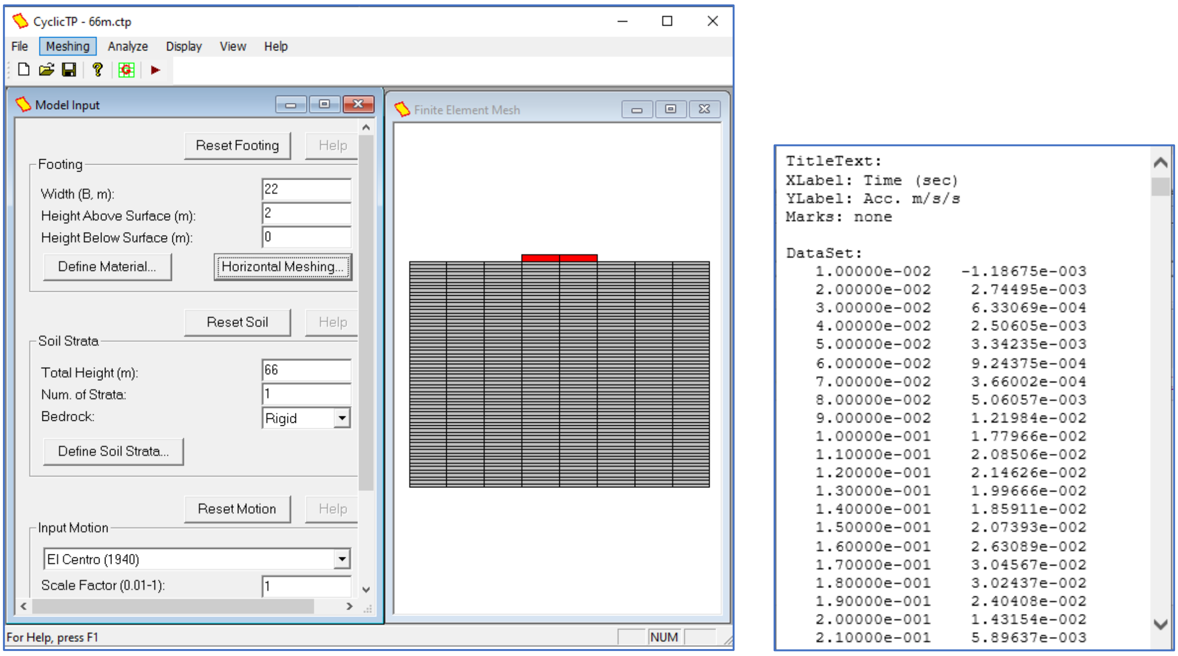

(a) CyclicTP's main window

(b) Response time history of foundation

Figure 9. First step SFI analysis using CyclicTP.

3.2. Effect of SSI on responses of liquid tank

In order to analyze two comparative models, replace $\ddot{\boldsymbol{u}}_{\boldsymbol{g}}$ for the fixed-base model for $\ddot{\boldsymbol{u}}_{\boldsymbol{1}}$ at the right side of Eq. (11) and input the system parameter and earthquake acceleration into Eq. (12) for the sway-rocking model. The data set obtained from CyclicTP represents the time-history accelerations of the foundation, as shown in Fig. 9(b).

Fig. 10 compares the results of the first step using various models. These results are the input data for the inertial interaction analysis of the second step. The second step is performed using the Simulink diagram shown in Fig. 7. The results of the second step are the liquid tank responses, as shown in Fig. 11, and Table 4 tabulates the peak values.

Table 4. Peak responses of the foundation and the liquid tank.

No.	Responses	Fixed base	Sway-rocking	Present	Error, $\frac{(5)-(2)}{(2)}$%	Error, $\frac{(5)-(3)}{(5)}$%
	(1)	(2)	(3)	(5)	(6)	(7)
1	$\ddot{u}_1$ (m/s^2)	3.19	5.64	5.20	63.01%	8.46%
2	x_i (10^{-4} m)	7.14	10.97	12.18	70.53%	9.93%
3	x_c (10^{-1} m)	1.34	1.37	1.67	24.74%	17.96%
4	M (10^7 Nm)	2.35	3.23	4.02	70.92%	19.65%
5	Q (10^7 N)	0.55	0.75	0.93	68.17%	19.35%

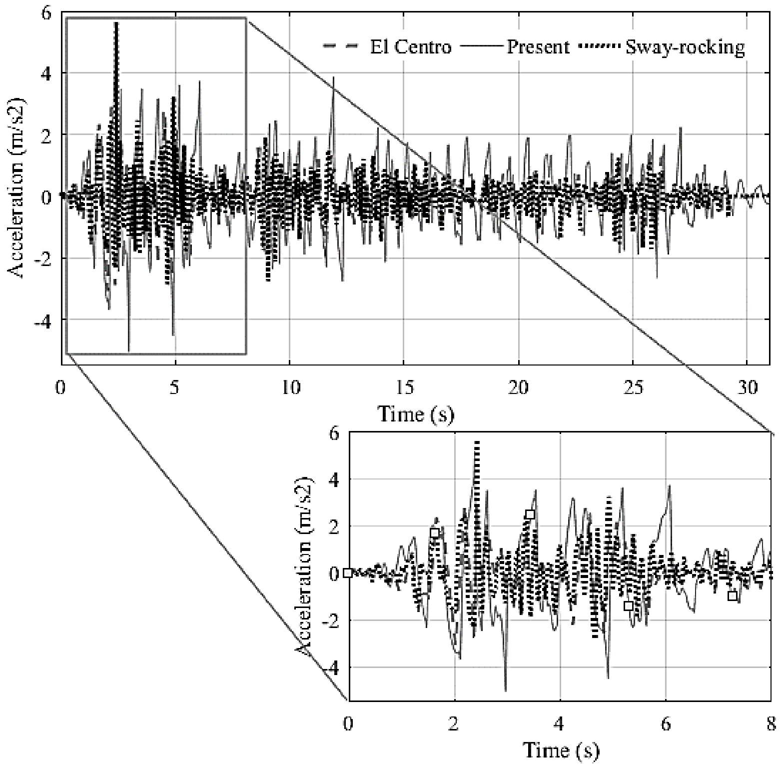

Figure 10. Time-history acceleration foundations: present model ($\ddot{\boldsymbol{u}}_{\boldsymbol{1}}$), sway-rocking model, and fixed-base model (El Centro, $\ddot{\boldsymbol{u}}_{\boldsymbol{g}}$).

The tank foundation's acceleration is higher than that of the fixed-base model, El Centro (1940); see Fig. 10 and row 1 of Table 4. The peak acceleration of the tank foundation is higher than that of the fixed-base and sway-rocking models, at 63.01% and 8.46%, respectively. Since both the proposed model and the sway-rocking model take soil-foundation interaction into account, the analysis results between the two models are similar (see Fig. 11 and column 7 of Table 4).

As illustrated in Fig. 11(a), the impulsive mass displacements increased significantly as a result of the SSI effect, whereas Fig. 11(b) shows that the convective mass displacements of the three models were similar. In line with Farajian's research [19], the convective response has a comparatively long period. For instance, the maximum displacements of the impulsive and convective masses increased by 70.53% and 24.74%, respectively, in comparison to a fixed-base model (see column 6 of Table 4).

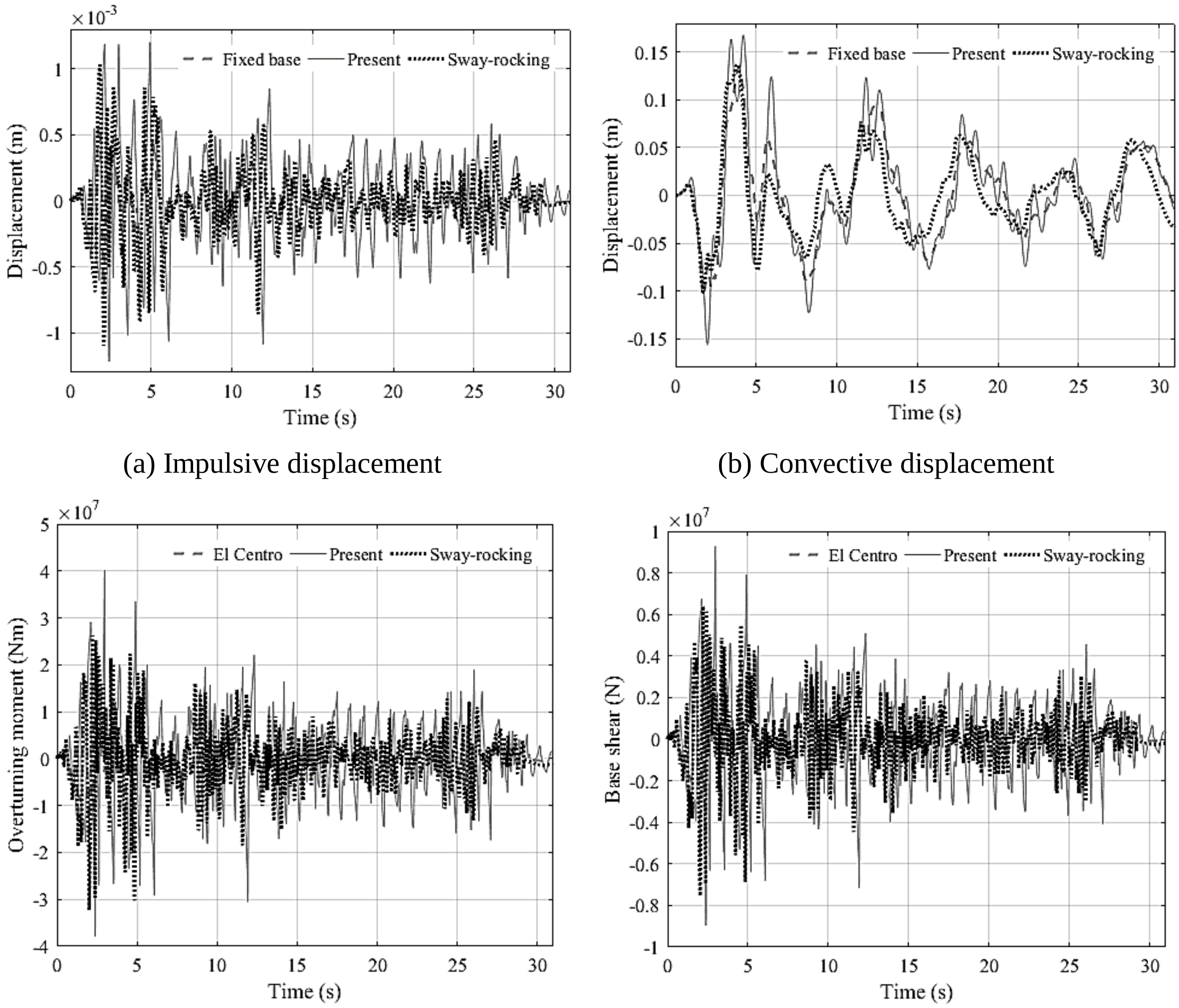

(a) Impulsive displacement

(b) Convective displacement

(c) Overturning moment

(d) Base shear force

Figure 11. Comparison of the responses obtained by two-step method and fixed base analysis.

Furthermore, the proposed method enables the computation of the structural base shear force (Q) and overturning moment (M) using the formulas $Q = k_c x_c + c_c \dot{x}_c + k_i x_i + c_c \dot{x}_i$ and $M = (k_c x_c + c_c \dot{x}_c) h_c + (k_i x_i + c_c \dot{x}_i) h_i$ [19]. The SSI increased the overturning moment and base shear force by 70.92% and 68.17%, respectively; see Figs. 11(c-d) and column 6 of Table 4. Column 7 of Table 4 shows that there are only 20% deviations from the sway-rocking model.

3.3. The system's response to different grounds

CyclicTP not only analyzes effectively with sandy soils but also with clay soils. The software has predefined these soils, but users can also define a new soil with particular characteristics. Moreover, the software allows the ground to be divided into a maximum of ten separate strata, with multiple layers of equal depth being created within each stratum.

This section uses these characteristics to examine clay strata as well as multiple strata with profiles in Table 5. The good soils suitable for shallow foundations are those with the properties of soil indicated in Table 2. Similar to the previous sections, two steps of seismic analysis are performed. Fig. 12 displays the time-history accelerations of foundations to various grounds, and Table 5 lists the maximum values. The analysis's results show that the responses of the liquid tanks and foundation accelerations are influenced by soil strata.

Table 5. The soil profiles and peak responses.

No.	Soil stratum	$\ddot{u}_1$ (m/s^2)	x_i (10^{-4} m)	x_c (10^{-1} m)	M (10^7 Nm)	Q (10^7 N)
1	66 m - stiff clay	1.71	5.42	6.42	1.60	0.34
2	66 m - medium clay	1.08	3.60	4.67	1.08	0.22
3	66 m - multiple strata: • Dense sand (6 m) • Medium clay (10 m) • Stiff clay (50 m)	1.02	3.43	3.96	1.11	0.24

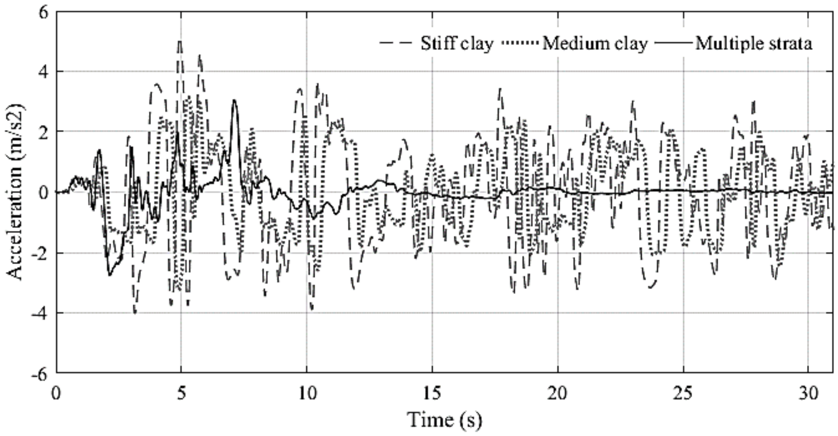

Figure 12. Time-history accelerations of foundations with various soil strata.

4. CONCLUSIONS

The paper proposed a two-step method based on the superposition theorem to analyze the seismic responses of the SFTL system. Using the finite-element program, SFI analysis is performed in the first step. The liquid tank model in LMP is used to analyze the second step. SFI analysis is performed in the first step using the finite-element program, the free download tool CyclicTP was used to analyze this paper. In this study, soil-shallow foundation interaction was analyzed using CyclicTP, a free download tool. In dense sand homogeneous soil, fixed-base model responses were 24–70% higher than those of the proposed method. In the meantime, variations from the sway-rocking model were found to be less than 20%. The paper also investigated grounds composed of clay soils and multiple soil strata. In addition to ground behaviors and the stress-strain relationships of the tank wall, future experimental research is recommended. These studies also need to take into account the geometric nonlinearity of the soil-foundation system, which is the foundation bottom sliding and separating from the ground.

REFERENCES

[1]. Y. M. A. Hashash, K. Karina, D. Koutsoftas, N. O'Riordan. Seismic design considerations for underground box structures, In Earth retention conference 3, Geotechnical Special Publication Bellevue, (2010) 620-637. https://doi.org/10.1061/41128(384)64

[2]. C. G. Lai, M. Martinelli., Soil-structure interaction under earth-quake loading: theoretical framework, In ALERT Doctoral School, 2013, 3.

[3]. N. NIST, Soil-structure-interaction for building structures (NIST GCR 12-917-21), National Institute of Standards and Technology, 2012, Gaithersburg.

[4]. E. Kausel, R. V. Whitman, J. P. Morray, F. Elsabee, The spring method for embedded foundations, Nuclear Engineering and Design, 48 (1978) 377-392. https://doi.org/10.1016/0029-5493(78)90085-7

[5]. A. A. Seleemah, M. El-Sharkaw, Seismic analysis and modeling of isolated elevated liquid storage tanks, Earthquakes and Structures, 2 (2011) 397-412. http://dx.doi.org/10.12989/eas.2011.2.4.397

[6]. A. A. Seleemah, M. El-Sharkawy, Seismic response of base isolated liquid storage ground tanks, Ain Shams Engineering Journal, 2 (2011) 33–42. https://doi.org/10.1016/j.asej.2011.05.001

[7]. R. A. M. A. Z. A. N. Livaoglu, A. Dogangun, Effect of foundation embedment on seismic behavior of elevated tanks considering fluid–structure-soil interaction, Soil Dynamics and Earthquake Engineering, 27 (2007) 855-863. https://doi.org/10.1016/j.soildyn.2007.01.008

[8]. R. Zhang, S. Chu, K. Sun, Z. Zhang, H. Wang, Effect of the directional components of earthquakes on the seismic behavior of an unanchored steel tank, Applied Sciences, 10 (2020). https://doi.org/10.3390/app10165489

[9]. H. V. Quan, Seismic analysis of liquid-storage tank with elastic response spectrum of TCVN 9386:2012 specification, Transport and Communications Science Journal, 73 (2022) 127-139 (in Vietnamese). https://doi.org/10.47869/tcsj.73.2.3

[10]. S. K. Saha, V. A. Matsagar, A. K. Jain, Earthquake response of base-isolated liquid storage tanks for different isolator models, Journal of Earthquake and Tsunami, 8 (2014). https://doi.org/10.1142/S1793431114500134

[11]. O. Miguel, T. Larkin, N. Chouw, Comparison between standards for seismic design of liquid storage tanks with respect to soil-foundation-structure interaction and uplift, Bulletin of The New Zealand Society for Earthquake Engineering, 45 (2012) 40-46. https://doi.org/10.5459/bnzsee.45.1.40-46

[12]. M. K. Kim, Y. M. Lim, S. Y. Cho, K. H. Cho, K. W. Lee, Seismic analysis of base-isolated liquid storage tanks using the BE–FE–BE coupling technique, Soil Dynamics and Earthquake Engineering, 22 (2002) 1151-1158. https://doi.org/10.1016/S0267-7261(02)00142-2

[13]. P. K. Malhotra, T. Wenk, M. Wieland, Simple procedure for seismic analysis of liquid-storage tanks, Structural Engineering International, 10 (2018) 197-201. https://doi.org/10.2749/101686600780481509

[14]. M. K. Shrimali, R. S. Jangid, Non-linear seismic response of base-isolated liquid storage tanks to bi-directional excitation, Nuclear Engineering and design, 217 (2002) 1-20. https://doi.org/10.1016/S0029-5493(02)00134-6

[15]. M. K. Shrimali, R. S. Jangid, Seismic response of liquid storage tanks isolated by sliding bearings, Engineering structures, 24 (2002) 909-921. https://doi.org/10.1016/S0141-0296(02)00009-3

[16]. M. K. Shrimali, R. S. Jangid, Seismic analysis of base-isolated liquid storage tanks, Journal of Sound and Vibration, 275 (2004) 59-75. https://doi.org/10.1016/S0022-460X(03)00749-1

[17]. API, Welded steel tanks for oil storage, in API Standard 650, 11th Ed., American Petroleum Institute, 2007.
[18]. NZSEE, Seismic design of storage tanks-recommendations of a study group of the New Zealand society for earthquake engineering, in NZSEE Standard, 2009.
[19]. M. Farajian, M. I. Khodakarami, D. P. N. Kontoni, Evaluation of soil-structure interaction on the seismic response of liquid storage tanks under earthquake ground motions, Computation, 5 (2017). https://doi.org/10.3390/computation5010017
[20]. T. Larkin. Seismic response of liquid storage tanks incorporating soil structure interaction. Journal of Geotechnical and Geoenvironmental Engineering, 134 (2008) 1804-1814. https://doi.org/10.1061/(ASCE)1090-0241(2008)134:12(1804)
[21]. T. Larkin, Earthquake response of liquid storage tanks on layered sites, in Soil-Foundation-Structure Interaction, 1st ed., CRC Press, 2010, pp. 155-162.
[22]. Y. Lyu, J. Sun, Z. Sun, L. Cui, Z. Wang, Simplified mechanical model for seismic design of horizontal storage tank considering soil-tank-liquid interaction, Ocean Engineering, 198 (2020). https://doi.org/10.1016/j.oceaneng.2020.106953
[23]. H. V. Quan, P. N. Bay, Seismic analysis of liquid-storage tank considering soil-structure interaction with macro element, Transport and Communications Science Journal, 75 (2022) 833-844. (in Vietnamese). https://doi.org/10.47869/tcsj.73.8.7
[24]. H. V. Quan, Effects of liquid height and soil deformation on responses of liquid storage tanks under seismic loading in Vietnam, TNU Journal of Science and Technology, 227 (2022) 197 – 206 (in Vietnamese). https://doi.org/10.34238/tnu-jst.6649
[25]. H. V. Quan, N. T. H. Phan, Seismic analysis of a soil-liquid tank system using MATLAB Simulink, Journal of Transportation Science and Technology, 12 (2023) 22-31 (in Vietnamese). https://www.doi.org/10.55228/JTST.12(5).22-31
[26]. SSI Simulation tools. http://www.soilquake.net/, (accessed 13 May 2023).
[27]. A. Malekjafarian, S. Jalilvand, P. Doherty, D. Igoe, Foundation damping for monopile supported offshore wind turbines: A review, Marine Structures, 77 (2021). https://doi.org/10.1016/j.marstruc.2021.102937
[28]. H. Inaba, M. Nagata, K. J. Miyake, A. M. Kabir, A. Kakugo, K. Sada, K. Matsuura, Cyclic Tau-derived peptides for stabilization of microtubules, Polymer journal, 52 (2020) 1143-1151. https://doi.org/10.1038/s41428-020-0356-3
[29]. A. K. Verma, S. Mohanty, Finite element analysis of foundation on layered and homogeneous soil deposit under dynamic loading, in Geohazards, (2021) 481-493.
[30]. A. K. Ram, S. Mohanty, Numerical analysis of layered soil-ash-foundation system, In Proceedings of the 7th Indian Young Geotechnical Engineers Conference, 2022, Springer, pp. 339-351.
[31]. A. K. Ram, A. Verma, S. Mohanty, 1D, 2D, and 3D seismic response analysis of shallow and deep foundation resting on stratified soil deposit, In Indian Geotechnical Conference, (2023) 377-389.
[32]. Soil Properties. http://www.soilquake.net/cyclic1d/parameters.html, (accessed 13 May 2023).
[33]. R. D. Holtz, W. D. Kovacs, An introduction to geotechnical engineering, Prentice Hall, Englewood Cliffs, New Jersey, 1981.
[34]. El Centro Earthquake Page. http://www.vibrationdata.com/elcentro.htm, (accessed 13 May 2023).
[35]. A. K. Chopra, Dynamics of structures, Prentice-Hall, New Jersey, 1995.